

周波数領域等化を用いた DS-CDMA 伝送における タイミングずれによる影響

劉 楽[†] 陳 樵毅 安達 文幸[‡]

東北大学大学院工学研究科電気・通信工学専攻 〒980-8580 仙台市青葉区荒巻字青葉 6-6-05

E-mail: [†]liule@mobile.ecei.tohoku.ac.jp, [‡]adachi@ecei.tohoku.ac.jp

あらまし 周波数選択性フェージングチャネルにおける直接拡散符号分割多重アクセス(DS-CDMA)伝送に有効な等化技術として、周波数領域等化(FDE)が最近注目を浴びている。実システムでは、ルートナイキスト送受信フィルターが信号帯域制限のために使われている。このため、受信タイミングずれにより符号間干渉(ISI)が生じ、伝送特性が劣化する。本論文では、受信タイミングずれがある場合について、周波数選択性フェージング環境下における FDE を用いた DS-CDMA のビット誤り率(BER)の理論解析を示し、計算機シミュレーションにより理論解析の妥当性を確認している。受信タイミングずれがある場合は、受信信号時間領域で拡散してしまい、受信信号を含むように、フーリエ変換のための観測窓をシフトしなければならないこと、誤り率を最少化する最適ロールオフファクターはほぼ 0.2 になることを明らかにしている。

キーワード DS-CDMA, 周波数領域等化, タイミングずれ, ナイキスト送受信フィルター。

Impact of Timing Error on DS-CDMA with Frequency-domain Equalization

Le LIU[†], Chiao-Yi CHEN and Fumiyuki ADACHI[‡]

Dept. of Electrical and Communication Engineering, Graduate School of Engineering,

Tohoku University, 6-6-05, Aza-Aoba, Aramaki, Aoba-ku Sendai 980-8580, JAPAN

E-mail: [†]liule@mobile.ecei.tohoku.ac.jp, [‡]adachi@ecei.tohoku.ac.jp

Abstract Recently, the frequency-domain equalization (FDE) has been attracting much attention since it is an effective equalization technique for direct-sequence code division multiple access (DS-CDMA) signal transmission in a frequency-selective fading channel. In practical systems, the square-root Nyquist transmit and receive filters are used for the bandwidth limitation of the transmitted signals. The presence of timing error produces the inter-symbol interference (ISI) and thus degrades the transmission performance. In this paper, we present a theoretical analysis on the bit error rate (BER) performance of DS-CDMA using FDE in the presence of timing error and the analysis is confirmed by computer simulation. In the presence of timing error, the received signal spreads in the time domain and the FFT window should be shifted to contain most of desired signal components. The optimum rolloff factor that minimizes the average BER is around 0.2.

Keyword DS-CDMA, frequency-domain equalization, timing error, Nyquist filter

1. INTRODUCTION

A wireless channel is composed of many propagation paths with different time delays, producing frequency-selective fading [1]. Direct-sequence code division multiple access (DS-CDMA) can exploit the channel frequency-selectivity by the use of a rake receiver that resolves the propagation paths with different time delays and coherently combines them to achieve the path-diversity effect for achieving data transmissions of up to a few Mbits/s [2][3]. However, for high-speed transmission, the bit error rate (BER) performance with coherent rake combining may significantly degrade due to severe interpath interference (IPI). Recently, multicarrier CDMA (MC-CDMA) has been attracting much attention for broadband wireless data transmission in a severely frequency-selective channel [4]. Although MC-CDMA can make use of frequency selectivity by using frequency-domain equalization (FDE), it suffers from large peak-to-average power ratio (PAPR). More recently, it was shown that the use of FDE based on the

minimum mean square error (MMSE) criterion improves the bit error rate (BER) performance of DS-CDMA and achieves a similar performance to MC-CDMA [5].

However, unlike MC-CDMA, DS-CDMA needs transmit/receive filters to limit the signal bandwidth. The presence of timing error produces inter-symbol interference (ISI). In this paper, we develop a theoretical foundation for the BER performance of DS-CDMA using MMSE-FDE in the presence of timing error. The remainder of this paper is organized as follows. Section 2 presents the transmission system model of DS-CDMA using FDE. Section 3 discusses the impact of timing error on the channel estimation. In section 4, an expression for the conditional BER is derived for the given set of channel gains and timing error. The average BER performance is evaluated by a Monte-Carlo numerical computation method using the derived conditional BER and is confirmed by computer simulation in Sect. 5. Section 6 concludes the paper.

2. TRANSMISSION SYSTEM MODEL

Figure 1 shows the transmitter and receiver structures of multicode DS-CDMA with FDE. Throughout the paper, a chip-spaced discrete-time representation of signals is used.

2.1 Transmitted Signal Representation

The bit sequence to be transmitted is data-modulated and then serial-to-parallel (S/P) converted to C parallel symbol streams, $\{d_u(n); u=0\sim C-1\}$. The u th symbol stream is spread by the orthogonal spreading code $\{c_u(t); t=0\sim SF-1\}$ with spreading factor SF ($SF \geq C$). The sum of C parallel chip sequences is multiplied by a scrambling sequence to form the orthogonal multicode DS-CDMA signal, which is divided into blocks of N_c chips each. The chip block is expressed as

$$s(t) = \left[\sum_{u=0}^{C-1} d_u \left(\lfloor t/SF \rfloor \right) c_u(t \bmod SF) \right] c_{scr}(t) \quad (1)$$

for $t=0\sim N_c-1$ with $|d_u(n)| = |c_u(t)| = |c_{scr}(t)| = 1$, where $\lfloor x \rfloor$ represents the largest integer smaller than or equal to x . The N_g -chip cyclic prefix is inserted as a guard interval (GI). The GI-inserted transmit signal $\tilde{s}(t)$ can be expressed by using the equivalent lowpass representation as

$$\tilde{s}(t) = \sqrt{2E_c/T_c} s(t \bmod N_c) p_t(t) \quad (2)$$

for $t=-N_g\sim N_c-1$, where $p_t(t)$ is the square-root Nyquist transmit filter impulse response and E_c and T_c denote the chip energy and the chip duration, respectively.

2.2 Received Signal Representation

The propagation channel is assumed to be a chip-spaced L -path frequency-selective block-fading channel (the l th path time delay is l chips) and its discrete-time impulse response is given by

$$h(t) = \sum_{l=0}^{L-1} h_l \delta(t-l), \quad (3)$$

where $h_l(t)$ is the l th path complex channel gain with $\sum_{l=0}^{L-1} E[|h_l|^2] = 1$. The block fading means that the path gains remain constant over one block interval of N_c chips but change block-by-block.

At the receiver, the receive filter, whose impulse response $p_r(t)$ is $p_r(t) = p_t(-t)$, is used. The receiver filter output is sampled at the chip rate. The sampled sequence $\{r(t); t=-N_g\sim N_c-1\}$ is expressed as

$$r(t) = \sum_{l=0}^{L-1} \sum_{n=-\infty}^{\infty} h_l \tilde{s}(n) p(t-l-\Delta t-n) + \eta(t), \quad (4)$$

where $\eta(t)$ is a zero-mean complex noise process having variance $2N_0/T_c$ with N_0 being the single-sided power spectrum density of the additive white Gaussian noise (AWGN), $p(t) = p_t(t) \otimes p_r(t)$ (\otimes denotes the convolution operation) is a root Nyquist filter and Δt ($|\Delta t| \leq 0.5$) is the timing error. $p(t)$ is given by

$$p(t) = \frac{\sin(\pi t)}{\pi t} \frac{\cos(\pi \alpha t)}{1 - (2\alpha t)^2}, \quad (5)$$

where α ($0 \leq \alpha \leq 1$) is the rolloff factor. Using Eq. (3), Eq. (4) can be rewritten as

$$r(t) = \sum_{\tau=-\infty}^{+\infty} \bar{h}_\tau \tilde{s}(t-\tau) + \eta(t), \quad (6)$$

where \bar{h}_τ is given by

$$\bar{h}_\tau = \sum_{l=0}^{L-1} h_l p(\tau-l-\Delta t). \quad (7)$$

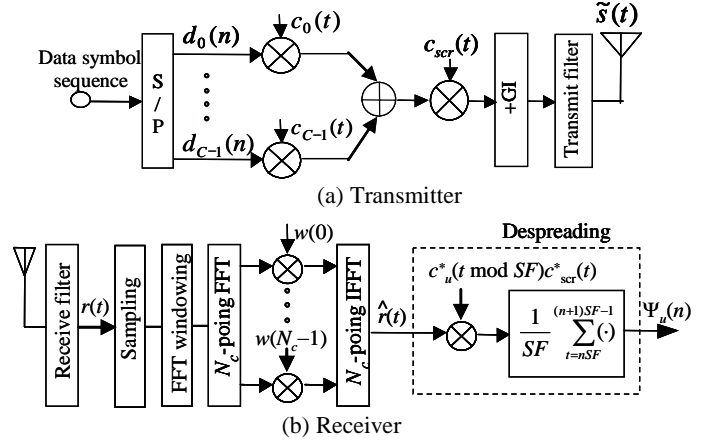


Fig. 1 Transmitter/receiver structure for DS-CDMA with FDE.

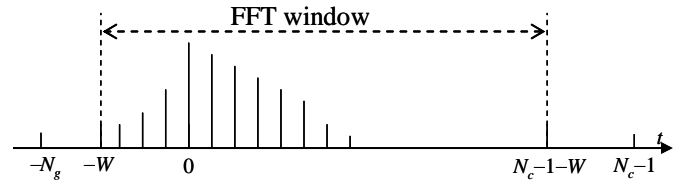


Fig. 2 FFT window.

2.3 FDE

Without timing error, the received signal in the time interval $t=-N_g\sim 0$ is removed to avoid the inter-block interference (IBI) and then, N_c -point FFT is applied to the GI removed received signal $\{r(t); t=0\sim N_c-1\}$ to transform into the frequency-domain signal $\{R(k); k=0\sim N_c-1\}$. However, in the presence of timing error, since the overall (transmit/receive filters+channel) impulse response, defined as

$$\bar{h}(t) = \sum_{\tau=-\infty}^{+\infty} \bar{h}_\tau \delta(t-\tau), \quad (9)$$

spreads more than the original response, the N_c -point FFT window should be shifted by W chips as shown in Fig. 2. W is an important design parameter.

The received signal $\{r(t); t=-W\sim N_c-1-W\}$ is transformed into the frequency-domain signal $\{R(k); k=0\sim N_c-1\}$. $R(k)$ is given by

$$R(k) = \sum_{t=0}^{N_c-1} r(t-W) \exp\left(-j2\pi k \frac{t}{N_c}\right), \quad (10)$$

$$= \sqrt{2E_c/T_c} S(k) \bar{H}(k) + \Pi(k)$$

where $S(k)$, $\bar{H}(k)$, and $\Pi(k)$ are the k th frequency component of $s(t)$, the Fourier transform of $\bar{h}(t)$, and the noise with variance $(2N_0/T_c)N_c$, respectively. They are given by

$$\begin{cases} S(k) = \sum_{t=0}^{N_c-1} s(t) \exp\left(-j2\pi k \frac{t}{N_c}\right) \\ \bar{H}(k) = \exp\left(-j2\pi k \frac{W}{N_c}\right) \sum_{\tau=-\infty}^{+\infty} \bar{h}_\tau \exp\left(-j2\pi k \frac{\tau}{N_c}\right) \\ \Pi(k) = \sum_{t=0}^{N_c-1} \eta(t-W) \exp\left(-j2\pi k \frac{t}{N_c}\right) \end{cases} \quad (11)$$

One-tap FDE is performed as

$$\hat{R}(k) = w(k)R(k) = \sqrt{2E_c/T_c} S(k) \hat{H}(k) + \hat{\Pi}(k), \quad (12)$$

where $\hat{H}(k)$ and $\hat{\Pi}(k)$ are given by

$$\begin{cases} \hat{H}(k) = w(k)\bar{H}(k) \\ \hat{\Pi}(k) = w(k)\Pi(k) \end{cases} \quad (13)$$

with $w(k)$ being the MMSE-FDE weight. $w(k)$ is given by [7]

$$w(k) = \frac{\bar{H}^*(k)}{|\bar{H}(k)|^2 + \left(\frac{C}{SF} \frac{E_s}{N_0}\right)^{-1}}, \quad (14)$$

where $(\cdot)^*$ denotes the complex conjugate operator.

2.4 Despreading

The frequency-domain signal $\{\hat{R}(k); k=0\sim N_c-1\}$ after FDE is transformed back to the time-domain signal $\{\hat{r}(t); t=0\sim N_c-1\}$ by N_c -point IFFT as

$$\hat{r}(t) = \frac{1}{N_c} \sum_{k=0}^{N_c-1} \hat{R}(k) \exp\left(j2\pi t \frac{k}{N_c}\right). \quad (15)$$

Finally, the decision variable $\Psi_u(n)$ of the n th data symbol in the u th data stream is obtained after despreading as

$$\Psi_u(n) = \frac{1}{SF} \sum_{t=nSF}^{(n+1)SF-1} \hat{r}(t) c_u^*(t \bmod SF) c_{scr}^*(t) \quad (16)$$

3. CHANNEL ESTIMATION

Coherent MMSE-FDE requires channel estimation (CE). Pilot-assisted channel estimation using time-multiplexed pilot blocks [8], [9] is considered. As shown in Fig. 3, one pilot chip block is followed by D data chip blocks in a frame.

The k th frequency component of the received pilot can be represented as

$$R_p(k) = \sqrt{2E_c/T_c} P(k) \bar{H}(k) + \Pi(k), \quad (17)$$

where $P(k)$ is the k th frequency component of the pilot $p(t)$ and is given by

$$P(k) = \sum_{t=0}^{N_c-1} p(t) \exp\left(-j2\pi k \frac{t}{N_c}\right). \quad (18)$$

The frequency-domain MMSE-CE [10], [11] can be used to obtain the channel estimate $\hat{H}(k)$ as

$$\hat{H}(k) = R_p(k) X^*(k) \quad (19)$$

with

$$X(k) = \frac{P(k)}{|P(k)|^2 + N_c(E_c/N_0)^{-1}}. \quad (20)$$

However, $\hat{H}(k)$ is noisy. To reduce the noise, we apply the delay-time domain windowing technique [12]. N_c -point IFFT is applied to transform $\{\hat{H}(k); k=0\sim N_c-1\}$ into the instantaneous channel impulse response $\{\hat{h}(\tau); \tau=0\sim N_c-1\}$ as

$$\hat{h}(\tau) = \frac{1}{N_c} \sum_{k=0}^{N_c-1} \hat{H}(k) \exp\left(j2\pi \tau \frac{k}{N_c}\right). \quad (21)$$

Then, N_c -point FFT is applied to obtain an improved channel estimate as

$$\tilde{H}(k) = \sum_{\tau=-\infty}^{+\infty} w_d(\tau) \hat{h}(\tau) \exp\left(-j2\pi \tau \frac{k}{N_c}\right), \quad (22)$$

where $w_d(\tau)$ is the delay time-domain window to reduce the noise. Without timing error (i.e., $\Delta t=0$), $\bar{h}(\tau)$ is present only within the GI (i.e., $\tau=0\sim N_g-1$) as shown in Fig. 4 (a). However, in the presence of timing error $\bar{h}(\tau)$ may spread beyond the GI as shown in Fig. 4(b). Therefore, we use the following rectangular window:

$$w_d(\tau) = \begin{cases} 1, & -W_{CE} \leq \tau \leq N_g - 1 + W_{CE} \\ 0, & \text{otherwise} \end{cases} \quad (23)$$

W_{CE} is an important design parameter. In the case of no timing error, $W_{CE}=0$.

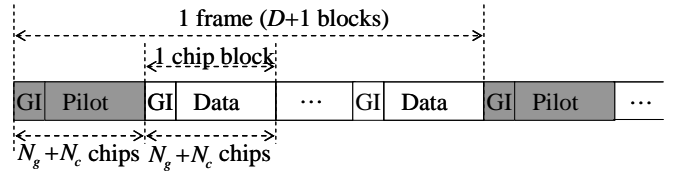


Fig. 3 Frame structure.

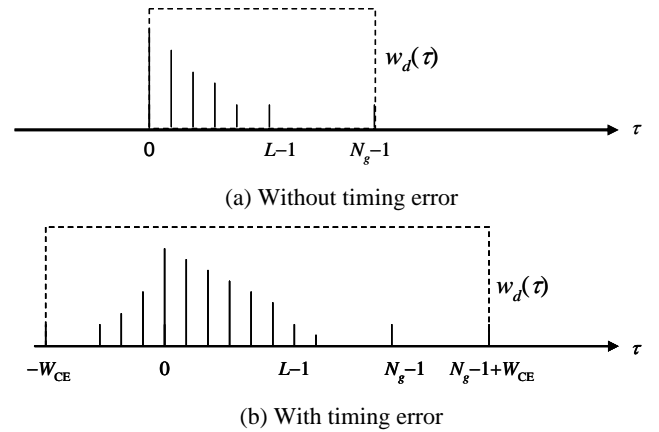


Fig. 4 Delay time-domain window.

4. BER ANALYSIS WITH IDEAL CHANNEL ESTIMATION

We assume quadrature phase shift keying (QPSK) modulation. Without loss of generality, we assume all "1"

transmission (i.e. $d_c(n) = (1 + j1)/\sqrt{2}$). Substituting Eqs. (1), (11), (12) and (15) into Eq. (16), we have

$$\Psi_u(n) = \sqrt{\frac{2E_c}{T_c}} \left(\frac{1}{N_c} \sum_{k=0}^{N_c-1} \hat{H}(k) \right) d_u(n) + \mu_{IBI}(n) + \mu_{ICI}(n) + \mu_{noise}(n), \quad (24)$$

where the first, second, third and fourth terms represent the desired signal component, the inter-block interference (IBI), the inter-chip interference (ICI) and the noise due to AWGN, respectively. Assuming that the GI is large enough, we consider the IBI is much smaller than ICI and hence μ_{IBI} can be neglected (i.e., $\mu_{IBI}=0$) in the analysis. μ_{ICI} and μ_{noise} are given by

$$\left\{ \begin{aligned} \mu_{ICI} &= \frac{1}{SF} \sum_{t=nSF}^{(n+1)SF-1} c_u^*(t \bmod SF) c_{scr}^*(t) \\ &\quad \times \frac{1}{N_c} \sum_{k=0}^{N_c-1} \hat{H}(k) \left[\sqrt{\frac{2E_c}{T_c}} \sum_{\substack{\tau=0 \\ \tau \neq t}}^{N_c-1} s(\tau) \exp\left(j2\pi k \frac{t-\tau}{N_c}\right) \right] \\ \mu_{noise} &= \frac{1}{SF} \sum_{t=nSF}^{(n+1)SF-1} c_u^*(t \bmod SF) c_{scr}^*(t) \\ &\quad \times \frac{1}{N_c} \sum_{k=0}^{N_c-1} \hat{\Pi}(k) \exp\left(j2\pi k \frac{k}{N_c}\right) \end{aligned} \right. \quad (25)$$

According to [7], μ_{ICI} can be approximated as a zero-mean complex-valued Gaussian noise. Consequently, the sum of μ_{ICI} and μ_{noise} can be treated as a new zero-mean complex-valued Gaussian noise μ with the variance given by

$$\sigma_\mu^2 = \sigma_{ICI}^2 + \sigma_{noise}^2, \quad (26)$$

where σ_{ICI}^2 and σ_{noise}^2 are the variances of μ_{ICI} and μ_{noise} , respectively, and are given by [7]

$$\left\{ \begin{aligned} \sigma_{ICI}^2 &= \frac{U}{SF} \frac{E_c}{T_c} \left[\frac{1}{N_c} \sum_{k=0}^{N_c-1} |\hat{H}(k)|^2 - \left| \frac{1}{N_c} \sum_{k=0}^{N_c-1} \hat{H}(k) \right|^2 \right] \\ \sigma_{noise}^2 &= \frac{1}{SF} \frac{N_0}{T_c} \left(\frac{1}{N_c} \sum_{k=0}^{N_c-1} |w(k)|^2 \right) \end{aligned} \right. \quad (27)$$

Since the ICI can be assumed to be circularly symmetric, the conditional BER for the given set of $\{H(k); k=0 \sim N_c-1\}$ can be expressed as [2]:

$$p_b \left(\frac{E_s}{N_0} \middle| \{H(k)\}, \Delta t \right) = \frac{1}{2} \operatorname{erfc} \left[\sqrt{\frac{1}{4} \gamma \left(\frac{E_s}{N_0} \middle| \{H(k)\}, \Delta t \right)} \right], \quad (28)$$

where $\operatorname{erfc}[x] = (2/\sqrt{\pi}) \int_x^\infty \exp(-t^2) dt$ is the complementary error function and $\gamma(E_s/N_0 | \{H(k)\})$ is the conditional SINR given by

$$\gamma \left(\frac{E_s}{N_0} \middle| \{H(k)\}, \Delta t \right) = \left(\frac{2E_c}{T_c} \left| \frac{1}{N_c} \sum_{k=0}^{N_c-1} \hat{H}(k) \right|^2 \right) / \sigma_\mu^2. \quad (29)$$

The average BER can be numerically evaluated by averaging Eq. (28) over all possible realizations of $\{H(k); k=0 \sim N_c-1\}$ and Δt .

5. NUMERICAL AND SIMULATION RESULTS

For numerical evaluation and computer simulation, we assume QPSK data modulation as assumed in Sect. 4. The numerical and simulation condition is shown in Table 1. We assume a full-loaded case ($C/SF=1$) since this provides the worst performance.

Table 1. Simulation condition

Transmitter	Block length	$N_c=256$
	GI length	$N_g=32$
	Spreading codes	Walsh codes
	Scrambling sequence	PN sequence
	Square-root raised cosine filter with rolloff factor α	
Rayleigh fading channel	No. of paths	$L=16$
	Time delay difference	$\tau=l$
	Power delay profile	Uniform
Receiver	Timing error	Uniformly distributed over $[-0.5, 0.5]$
	Square-root raised cosine filter with rolloff factor α	

5.1. Optimum chip shift W of FFT window

First, we conducted computer simulation to evaluate the BER performance with ideal CE in the presence of uniformly distributed timing error over $[-0.5, 0.5]$. Since we are assuming ideal channel estimation, the BER performance does not depend on W_{CE} . Fig. 5 shows a one-shot observation of $|\bar{h}(t)|$ for $\alpha=0, 0.22, 0.5$ and 1.0 . The overall (transmit/receive filters+channel) impulse response $\bar{h}(t)$ spreads outside the GI, thereby producing the IBI. Therefore, we need to optimize the chip shift W of the FFT window to minimize the IBI.

Figure 6 shows the BER dependency on W when $E_b/N_0=18$ dB. In the presence of timing error over $[-0.5, 0.5]$, the BER performance is very poor in the case of $\alpha=0$. If $\alpha \geq 0.22$, there exists the optimum W that minimizes the BER. The optimum W is broad and we set $W=10$ in the following simulation.

5.2. BER performance with ideal CE

First, we show the impact of α on the BER performance when the average $E_b/N_0=18$ dB in Fig. 7, where both the theoretical and simulated BER performances with ideal CE in the presence of uniformly distributed timing error are plotted. As α decreases from 1 to around 0.2, the BER performance improves since the ICI reduces. The numerical result agrees very well with the simulated one. However, as α reduces further, the simulated BER starts to increase due to the increasing IBI. However, it is observed that the theoretical BER consistently decreases. This is because the IBI was neglected in our theoretical analysis. If $\alpha=0$, the large IBI results in very poor BER performance. $\alpha \approx 0.22$ is found to be optimum to achieve the best BER performance in the presence of timing error over $[-0.5, 0.5]$. If Δt is uniformly distributed over $[-0.25, 0.25]$ or $[-0.125, 0.125]$, the optimum α becomes a little smaller than $[-0.5, 0.5]$.

Fig. 8 plots the theoretical and simulated BER performances with ideal CE in the presence of uniformly

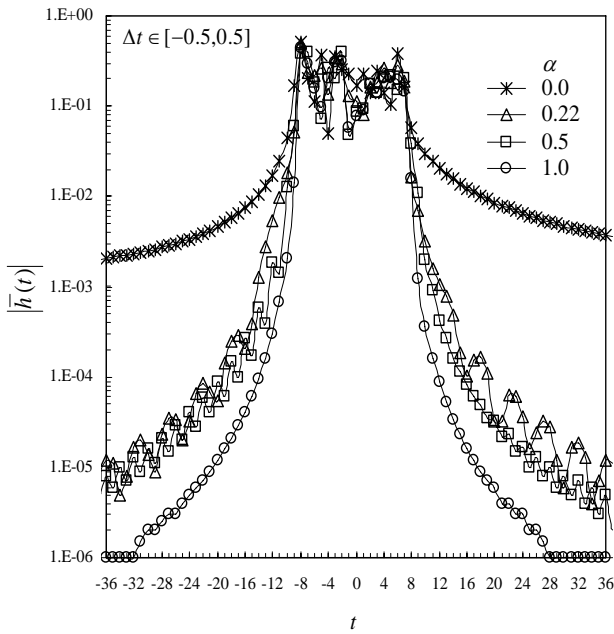


Fig. 5 Overall (transmit/receiver filters+channel) impulse response $\bar{h}(t)$.

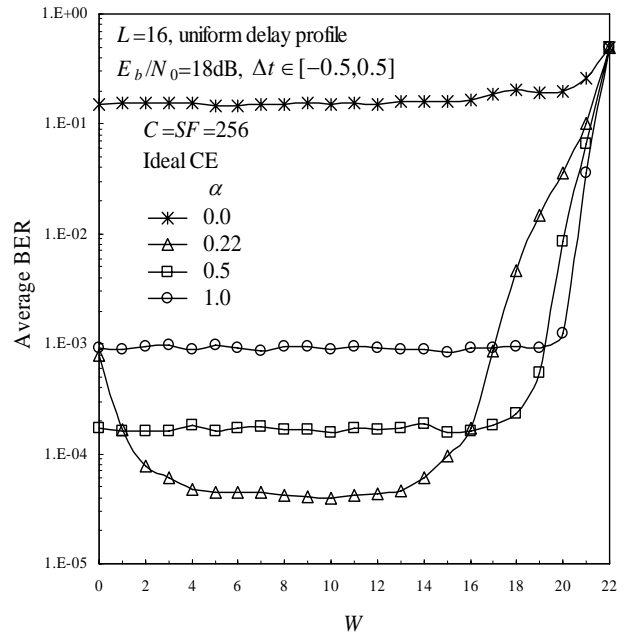


Fig. 6 Impact of W .

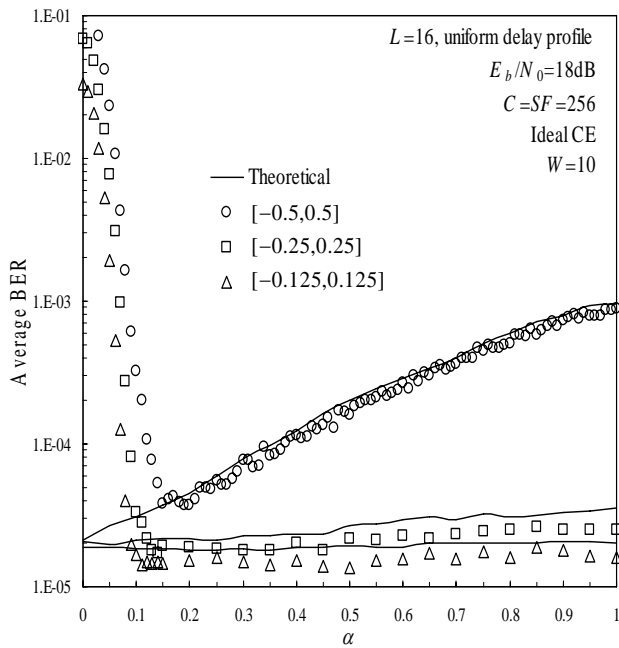


Fig. 7 Impact of α .

distributed timing error over $[-0.5, 0.5]$ as a function of E_b/N_0 . The BER performance with $\alpha=0$ is not plotted in Fig. 8, since it is very poor due to large IBI. For comparison, the BER performance without timing error is also plotted. With timing error, the BER performance degrades as expected from Fig. 7. It can be found that since the BER degrades

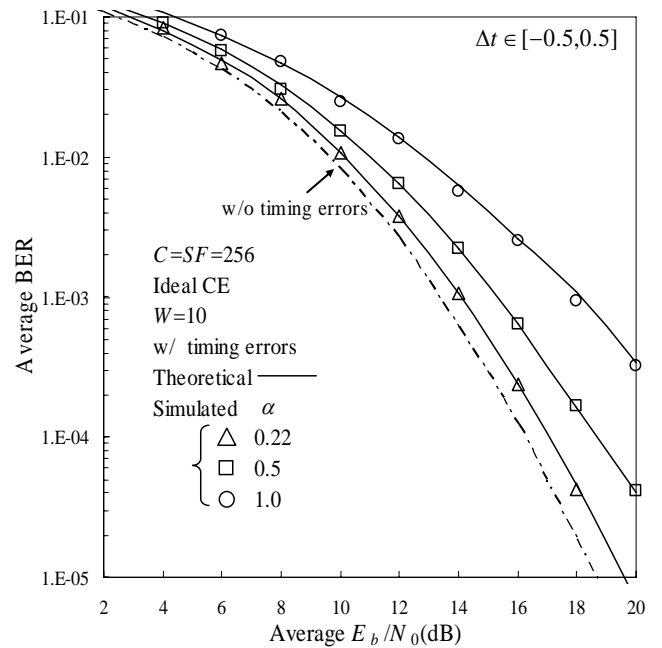


Fig. 8 Average BER performance with ideal CE.

significantly when $\alpha < 0.2$, $\alpha > 0.2$ should be used in practical systems. When $\alpha > 0.2$, the theoretically predicted BER is quite accurate and well agrees with the simulated one.

5.3. BER performance with pilot-assisted CE

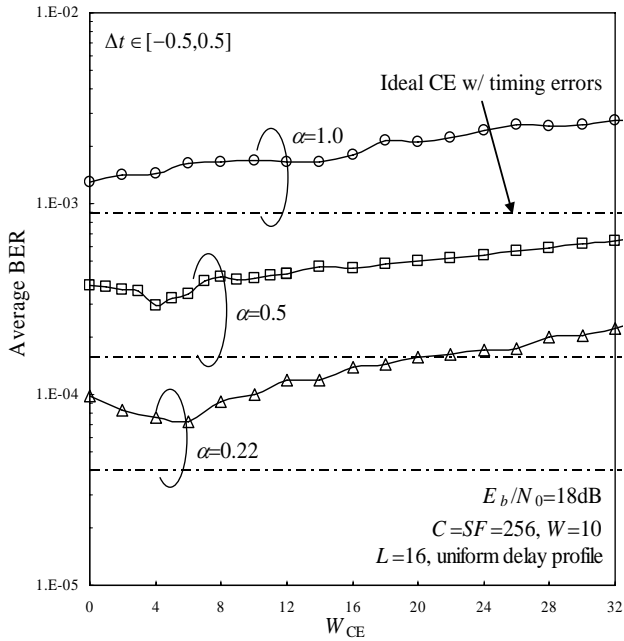


Fig. 9 Impact of W_{CE} .

Fig. 9 plots the BER dependency on W_{CE} when the average $E_b/N_0=18\text{dB}$ and Δt is uniformly distributed over $[-0.5, 0.5]$. The normalized maximum Doppler frequency $f_D(N_c+N_g)T_c=0.001$ is assumed (this corresponds to a terminal moving speed of 75km/h for a chip rate $1/T_c=100\text{Mcps}$ and 5GHz carrier frequency). One pilot block is followed by $D=15$ data chip blocks in a frame. For comparison, the BER performance with ideal CE in the presence of no timing error is also plotted. The accuracy of channel estimation depends on W_{CE} . If there is no timing error, $W_{CE}=0$ can be used; however, in the presence of timing error, MMSE-CE with $W_{CE}=0$ is not optimum. As W_{CE} is increased, the BER reduces. But if too large W_{CE} is used, the BER increases due to the increased noise in the channel estimate. The optimum W_{CE} depends on α and is found to be around $W_{CE}=6, 4$ and 0 for $\alpha=0.22, 0.5$ and 1.0 , respectively. The simulated BER performance with pilot-assisted CE is plotted for $\alpha=0.22$ in Fig. 10. The use of $W_{CE}=6$ provides the best BER performance over a wide range of average E_b/N_0 . The degradation of the required E_b/N_0 for $\text{BER}=10^{-4}$ from the case of ideal CE and no timing error is about 2dB .

6. CONCLUSION

In this paper, the theoretical foundation was developed for DS-CDMA using FDE in the presence of timing error. Since the overall (transmit/receive filters+channel) impulse response spreads in the presence of timing error, the FFT window should be shifted in order to contain the most of desired signal components. It was shown that the optimum window shift W is around $W=10$ irrespective of the transmit/receive filter rolloff factor α ($\approx 0\sim 1$). As for the rolloff factor α , the optimum α that minimizes the BER degradation is around 0.2 in the presence of timing error. Due to the timing error, the delay time-domain window used in the channel estimation for coherent FDE should also be extended

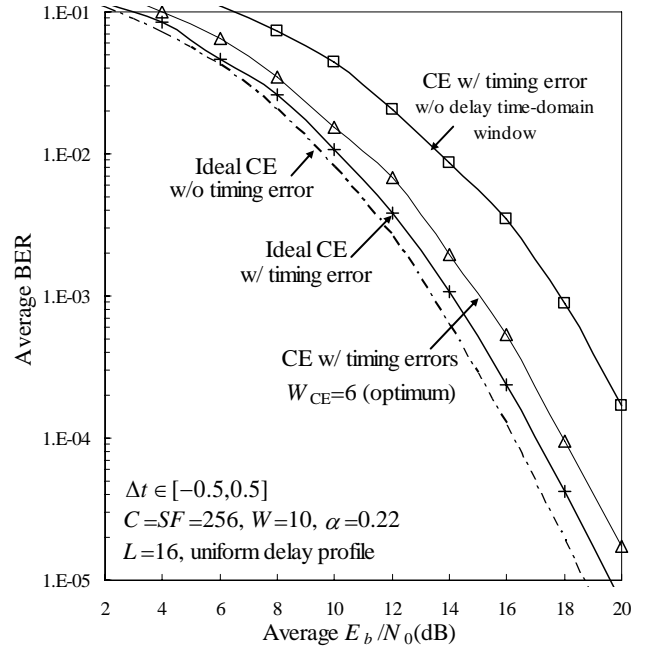


Fig. 10 Average BER performance with pilot-assisted CE.

by W_{CE} chips. We found by computer simulation that the optimum W_{CE} depends on α and is around $W_{CE}=6$ for $\alpha=0.22$.

REFERENCES

- [1] W.C., Jakes Jr, Ed, *Microwave mobile communications*, Wiley, Newyork, 1974.
- [2] J.G. Proakis, *Digital communications*, 2nd ed., McGraw-Hill, 1995.
- [3] F. Adachi, M. Sawahashi, and H. Suda, "Wideband DS-CDMA for next generation mobile communications systems," *IEEE Commun. Mag.*, Vol. 36, No. 9, pp. 56-69, Sep. 1998.
- [4] S. Hara and R. Prasad, "Overview of multicarrier CDMA" *IEEE Commun. Mag.*, vol. 35, no. 12, pp. 126-133, Dec. 1997.
- [5] F. Adachi, D. Garg, S. Takaoka and K. Takeda, "Broadband CDMA techniques," *IEEE Wireless Commun.*, vol. 12, no. 2, pp. 8-18, Apr. 2005.
- [6] H. Tomeba, K. Takeda, and F. Adachi, "BER performance of Single-Carrier Transmission in a channel having fractionally spaced time delays," *IEICE Report*, RCS2005-146, pp.131-136, Jan. 2005.
- [7] F. Adachi and K. Takeda, "Bit error rate analysis of DS-CDMA with joint frequency-domain equalization and antenna diversity combining," *IEICE Trans. Commun.*, vol. E87-B, no. 10, pp. 2991-3002, Oct. 2004.
- [8] H. Andoh, M. Sawahashi and F. Adachi, "Channel estimation filter using time-multiplexed pilot channel for coherent Rake combining in DS-CDMA mobile radio," *IEICE Trans. Commun.*, vol. E81-B, no. 7, pp. 1517-1526, July 1998.
- [9] S. Takaoka and F. Adachi, "Pilot-aided adaptive prediction channel estimation in a frequency-nonselctive fading channel," *IEICE Trans. Commun.*, vol. E85-B, no. 8, pp. 1552-1560, Aug. 2002.
- [10] K. Takeda and F. Adachi, "Pilot-assisted Channel Estimation for Based on MMSE Criterion for DS-CDMA with Frequency-domain Equalization," *Proc. IEEE VTC'05-Spring*, Stockholm, Sweden, 30 May-1 June 2005.
- [11] K. Takeda and F. Adachi, "SNR estimation for pilot-assisted frequency-domain MMSE channel estimation," *Proc. IEEE VTS APWCS*, Hokkaido University, Japan, 4-5 Aug. 2005.
- [12] J.-J. van de Beek, O. Edfors, M. Sandell, S. K. Wilson and P. O. Borjesson, "On channel estimation in OFDM systems," *Proc. IEEE VTC'95*, pp.815-819, Chicago, IL, July 1995.